Journal of Hydroscience and Hydraulic Engineering
Vol. 2, No. 2, November, 1984, pp.57-67.

NONLINEAR SEPARATION LAW OF RAINFALL AND ITS RELATION TO THE VARIABLE-SOURCE-AREA ANALYSED BY THE FILTER-SEPARATION AUTO-REGRESSIVE MODEL

By

Mikio Hino

Tokyo Institute of Technology, O-okayama, Meguro-ku, Tokyo, Japan

and

Masahiko Hasebe

Utsunomiya University, Ishii-cho, Utsunomiya, Japan

SYNOPSIS

By applying the authors' filter-separation AR method, the component rainfalls into subsystems of groundwater and interflow are estimated inversely from raw runoff time series. By analysing them, the nonlinear separation law of rainfall into components is derived and its relationship to the so-called "variable-source-area" concept is discussed. That is, the groundwater component rainfall, x_G, increases with the effective total rainfall x, reaches a certain limit, after then it is kept to a constant final infiltration rate into groundwater subsystem $(x_G)_f$ which is shown to be dependent on the preflood discharge rate q_A.

The temporal change of the second rainfall component, x_S, (inter-surface flow component) can be explained in terms of the effective source area a, a proportion of total basin area A. The variable-source-area ratio (of subsurface storm flow), A_r=a/A, is shown to be proportional to the basin storage, S.

INTRODUCTION

The generally accepted concept on the hydrological process is as follows; (i) rainfall infiltrates into the ground to fill the moisture defect as the initial loss and into deeper layer to become the groundwater flow, (ii) as the rainfall intensity increases and the infiltration rate from the upper porous layer exceeds the conductivity of lower less permeable layer and/or the soil moisture of lower layer becomes saturated, the infiltrated rainfall supplies the interflow and (iii) finally as moisture of the whole soil layer becomes saturated or as the rainfall intensity exceeds the infiltration capacity, the overland runoff begins.

Rainfall-runoff process is characterized by its strong nonlinearity. To explain the nonlinearity, several parametric models , such as the storage function model (Kimura (15) , Prasad (18)), kinematic wave model (Iwagaki (12), Eagleson (3)), the Volterra-Wiener expansion (Amorocho and Brandstetter (1), Hino et al (11), Hino and Nadaoka, (10)) , tank model (Sugawara (19, 20)), filter-separation AR model (Hino & Hasebe (5, 6, 9)), were proposed. Most of them are one-component input-output system. Sugawara's and the authors' models are composed of two or three subsystems supplied by multicomponent inputs (component rainfalls) into which the raw rainfalls are separated either through the cascade of tanks or by the nonlinear filters. Recently, the concept that the nonlinearity of rainfall-runoff process is caused not by the nonlinearity of subsystem itself, for instance by the overland flow, but mainly by the nonlinear-

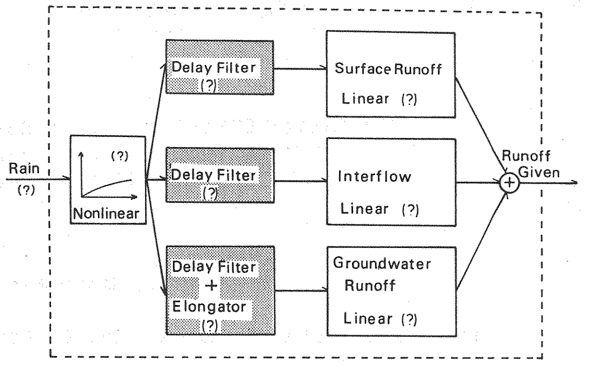

Fig.1 : Schematic diagram of a non-linear hydrologic system.

ity of the separation law of total rainfall into component rainfalls of subsystems seems to be acquiring a wide support (Kirkby (16), Kikkawa et al (14), Hino & Hasebe (5, 7, 9)).

One of the criticism on watershed-models is that most of them do not take into account the recently disclosed physical mechanism of hydrological processes such as those described in "Hillslope Hydrology" (Kirkby (16)). In the previous papers (Hino and Hasebe (5, 6, 7, 9)), we have proposed a new method of hydrological data anaysis ("filter-separation AR method"), which enables from runoff data alone to derive not only the hydrologic characteristics of subsystems (groundwater-flow, interflow and surface-flow) but also the rainfall component time series for each subsystem. In this paper, we analyse the time series of the inversely estimated rainfall components to discuss the nonlinear separation law of rainfall into subsystems and also to investigate the relation to the variable source area concept.

Component Separation of Raw Runoff Time Series

By plotting the recession period hydrograph of a flood record on a semi-logarithmic graph, a parameter of decay period T_c for groundwater-flow and interflow is determined

$$y(t) = y_0\, e^{-t/T_c} \tag{1}$$

where y_0 is a reference discharge rate and t is time measured from the reference time.

Then, properly selecting a parameter δ ($\delta \geq 2$; damping factor of an equivalent mass-dashpot-spring mechanical filtering system) a backward operating high-frequency cutoff numerical filter w(t) is designed by the relationship,

$$w(\tau) = \begin{cases} c_0 \exp(-\frac{1}{2}c_1\tau)\sinh[(\frac{1}{4}c_1{}^2-c_0)^{\frac{1}{2}}\tau]/(\frac{1}{4}c_1{}^2-c_0)^{\frac{1}{2}} & (\tau \geq 0) \\ 0 & (\tau<0) \end{cases} \tag{2}$$

where

$$c_0 = (\delta/T_c)^2, \qquad c_1 = \delta^2/T_c \tag{3}$$

Passing the raw runoff data through the filter, $w(\tau)$, the runoff time series y(t) are separated into components of groundwater flow, $y^{(1)}$, and inter-surface flow, $y^{(2)}$,

$$y^{(1)}(t) = \alpha\int^{t} w(t-\tau)y(\tau)d\tau \tag{4}$$

$$y^{(2)}(t) = y(t)-y^{(1)}(t) \tag{5}$$

where a weighting factor α is selected so as to retain $y^{(2)} \geq 0$ for all t.
If necessary, the inter-surface flow may be further divided into the interflow

$y^{(2)}$ and the surface flow $y^{(3)}$.

Although rainfall-runoff systems are generally speaking nonlinear, each subsystem thus separated is shown to be linear and expressible as shown in Fig.1 by the AR-model or ARX-model (auto-regressive model with exogenous input) (Hino and Hasebe (5, 6, 7, 9)).

Estimation of Component-Rainfall Time Series

The time-series of the separated runoff component for each subsystem are fitted to an AR-model;

$$y_i^{(l)}=a_1^{(l)}y_{i-1}^{(l)}+a_2^{(l)}y_{i-2}^{(l)}+\cdots+a_p^{(l)}y_{i-p}^{(l)}+b^{(l)}x_{i'}^{(l)}+\varepsilon_i^{(l)} \tag{6}$$

where $x^{(l)}$ and $y^{(l)}$ are the rainfall and runoff of the l-th subsystem, l=1,2 and 3 represent the subsystems of groundwater-flow, interflow and surface-flow respectively, $a^{(l)}$'s are the AR coefficients, the subscript i stands for the time step of $t=i\Delta t$, Δt being the time increment, the subscript i' means a delayed time step i'=i-lag and ε_i means a white noise. For brevity, the superscript l may be omitted hereafter, if there remains no apprehension of confusion. Considering a statonary state for a constant rainfall intensity and thus a constant discharge rate (for instance x=1(mm/h) and y=1(mm/h), the coefficient b is derived from the continuity relation as

$$b = 1-a_1-a_2-\cdots\cdots-a_p \tag{7}$$

If the units of x and y are different, a conversion factor λ should be multiplied to x; for instance if x and y are expressed by (mm/h) and (m^3/s), respectively, the conversion factor λ is given by

$$\lambda = A/3.6 \qquad [A:km^2] \tag{8}$$

where the drainage area A is expressed in unit of km^2.

Rearranging Eq. (6) and neglecting the noise term, the rainfall for the l-th subsystem is estimated from Eq. (9) or Eq.(10),

$$x_{i'}^{(l)}=(y_i^{(l)}-a_1^{(l)}y_{i-1}^{(l)}-a_2^{(l)}y_{i-2}^{(l)}\cdots\cdots-a_p^{(l)}y_{i-p}^{(l)})/(\lambda b^{(l)}) \tag{9}$$

or,

$$x_{i'}^{(l)}=[y_i^{(l)}-\lambda(h_2^{(l)}x_{i-2}^{(l)}+h_3^{(l)}x_{i-3}^{(l)}+h_4^{(l)}x_{i-4}^{(l)}+\cdots)]/(\lambda h_1^{(l)}) \tag{10}$$

where $h_i^{(l)}$'s mean the response function of the l-th subsystem for a unit impulse and are obtainable by the conversion of the AR coefficients, the symbol ^ is used to identify the inversely estimated values. Mathematically, the two expressions, Eqs. (9) and (10), are equivalent each other.

The effective total rainfalls are given by summing $x_{i'}^{(l)}$,

$$x_{i'} = \sum x_{i'}^{(l)} \tag{11}$$

As shown in the previous papers (Hino & Hasebe (5, 7, 9)), the inversely estimated rainfall time series compare well with the observed ones. Therefore, the inversely estimated component-rainfall time series may be believed to be true, although at the present time we could never verifify it since we cannot measure directly the component-rainfall time series.

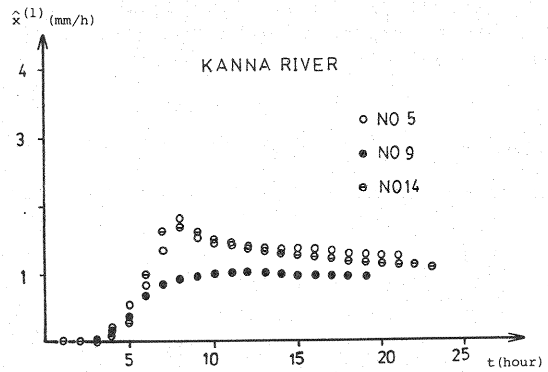

Fig.2 : Temporal variation of the inversely estimated rainfall component for groundwater flow corrected for the elongation effect, x_G.

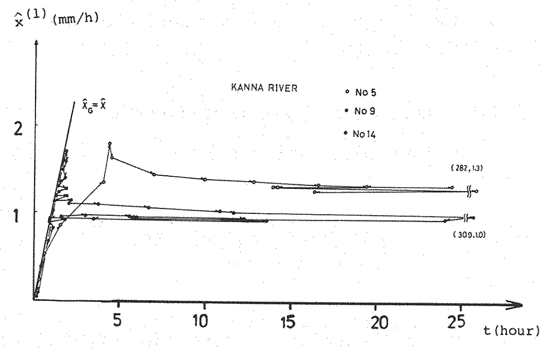

Fig.3 : Relation between the (inversely estimated) rainfall component for groundwater flow subsystem x_G and the effective total rainfall $x(=x^{(1)}+x^{(2)})$.

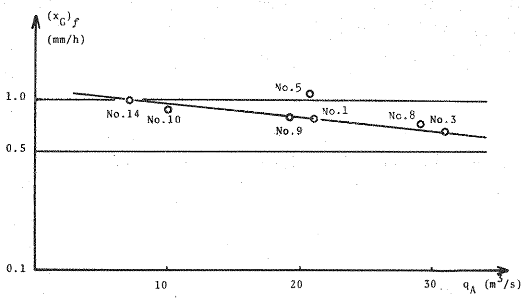

Fig.4 : Relation of the final infiltration rate to groundwater flow subsystem $(x_G)_f$ and the preflood discharge rate q_A.

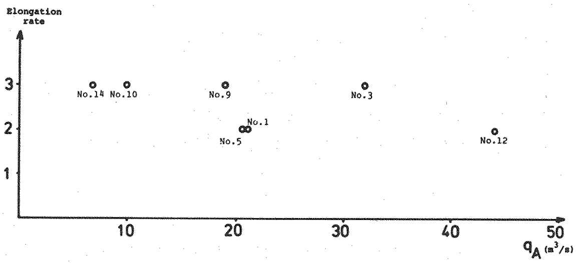

Fig.5 : Elongation ratio of rainfall component into groundwater subsystem against the preflood discharge rate, q_A.

NONLINEAR RAINFALL-SEPARATION LAW FOR GROUNDWATER FLOW

The data to be analysed are the flood records of the Kanna River, a tributary of the Tone River, Japan (Takenouchi, (21)). These data are one of the most reliable ones obtainable in Japan.

Rainfall on the ground-surface infiltrates into the lower layer of groundwater until the storage capacity of groundwater subsystem is filled or the infiltrating rainfall intensity exceeds the final infiltration rate into groundwater layer. (Note that this final infiltration rate into groundwater layer does not mean the conventional Hortonian final infiltration rate into surface soil cover, it being far greater than the former). In order to examine the infiltration law, the inversely estimated rainfall to the groundwater subsystem x_G $(=x^{(1)})$, which is corrected for the elongation effect to be discribed subsequently is plotted against time t and against the inversely estimated total effective rainfall intensity x (Figs. 2 and 3). As Fig. 3 shows, $x^{(1)}$ increases initially with the increase in x (i.e. at the initial stage, whole of the effective rainfalls being the groundwater rainfall component $x^{(1)}=x$) and finally reaches a final infiltration rate $(x_G)_f$. The increase of $x^{(1)}$ (and x) with time in the initial stage of Figs. 2 and 3 does not necessarily mean that the rainfall intensity increases with time but it is a reflection of the fact that

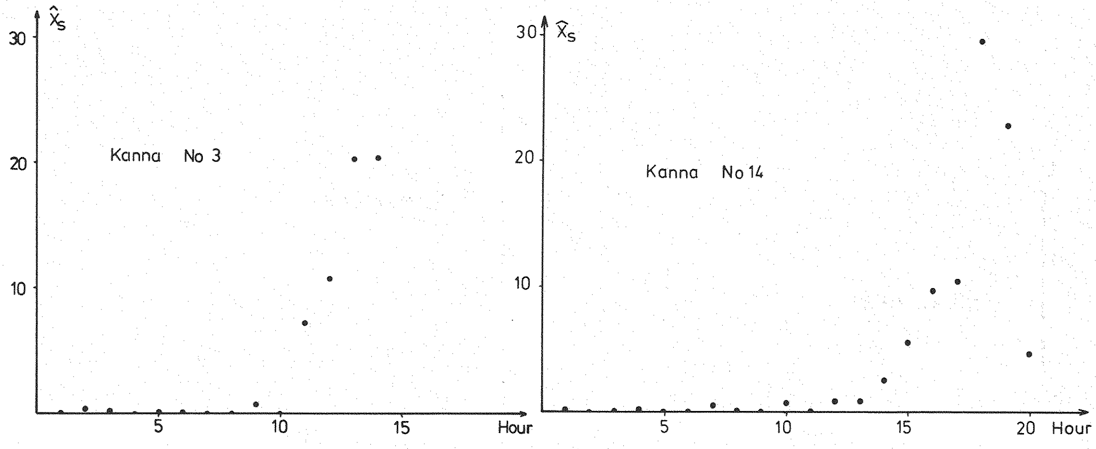

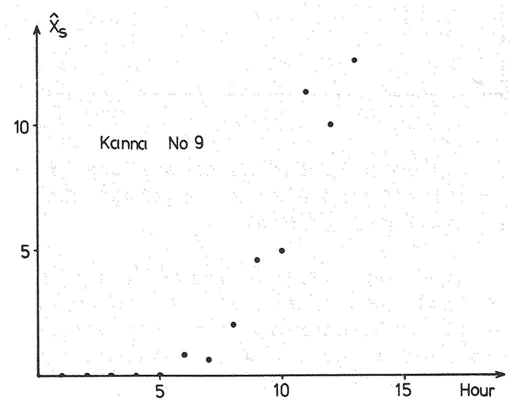

Fig.6 : Temporal variation of the inter-surface flow component of rainfall x_S.

the initial loss decreases with time.

The final infiltration intensity into the groundwater subsystem $(x_G)_f$ varies from case to case. Supposedly, it may be influenced by the soil moisture. The role of preflood discharge rate as an index of soil moisture has been pointed out, for instance, by Linsley et al (17), Iwai & Ishiguro (13) and Hino & Hasebe (8). Consequently, the final infiltration intensity into groundwater flow, $(x_G)_f$, is plotted against the preflood discharge rate, q_A, in Fig. 4 which indicates a good correlation.

By comparing the inversely estimated rainfall time series for groundwater subsystem with the observed ones, it is found that the durations of the estimated rainfall are elongated two or three times those of the observed one. This fact is explained as a result of the deformation of rainfall pattern during the infiltration process (Yamada, Hino and Fujita (22)). The elongation rate is plotted against q_A in Fig. 5. As the preflood discharge rate q_A becomes low, that is, as the soil moisture is low, rainfall will pass through a longer distance and the deformation of rainfall pattern may become large. The tendency is seen in Fig. 5. The data of x and $x^{(1)}$ $(=x_G)$ analysed in Figs. 2, 3 and 4 are the corrected ones.

RAINFALL-SEPARATION LAW FOR INTER-SURFACE FLOW COMPONENT AND VARIABLE SOURCE AREA-SUBSURFACE STORM FLOW CONCEPT

In our case, runoff data is separated into two components of groundwater $x^{(1)}$ $(=x_G)$ and inter-surface flow $x^{(2)}$ $(=x_S)$. The second (inversely estimated) rainfall component of inter-surface flow $x^{(2)}$, is processed in the same way as for x_G. However, any conclusive results have not been obtained. Figs. 6 and 7 are examples, showing no tendency. Since most of total rainfall x contributes to x_s; i.e. $x \cong x_s$, Fig.7 gives no information on the separation law of the observed real total rainfall. As for Fig.7, a short comment is added. As shown in Fig.3, for floods Nos.5, 9 and 14, rainfalls into groundwater component saturate at as low intensity as 2~5mm/h the relation between x and x_s seems to be nearly on a line with 1:1 slope.

Next, we considered that according to the concept that the direct runoff is the excess-rainfall, that is the rainfall which cannot infiltrate into or be stored in soils constitutes the direct runoff. Consequently, the so-to-speak

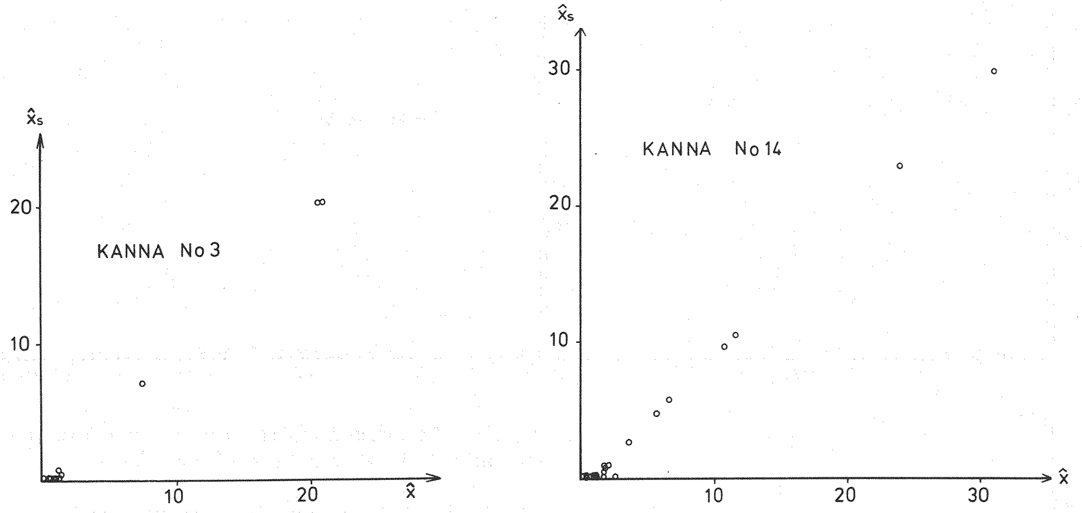

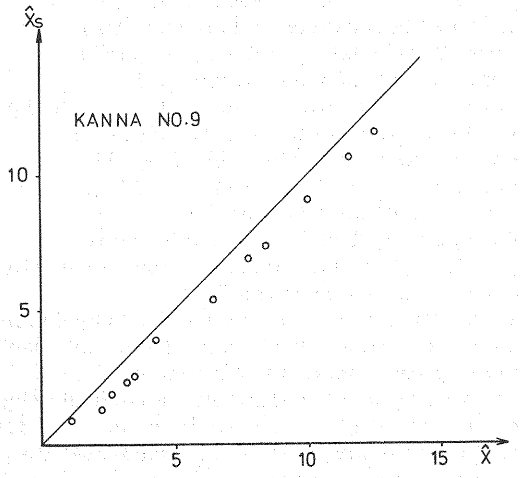

Fig.7 : Graph of the inter-surface flow component of rainfall, x_S, against the effective total rainfall x.

loss rate $x_l(t)=X(t)-x^{(1)}(t)-x^{(2)}(t)$, where X(t) means the total obserbed rainfall, will decrease smoothly with time depending on the soil moisture or the preflood discharge rate q_A. However, as shown in Fig.8, the result gave confusion.

After long consideration, an intuition has been awakened that these data may be explained by the so-called 'variable source area concept'. Suppose that X and $x^{(1)}$ ($=x_G$) are the real total rainfall intensity and its groundwater-flow component at time t, respectively. Then $X-x^{(1)}$ means the rainfall excess for groundwater infiltration process. However, according to the variable source area concept, a part of the drainage basin is effective to produce the surface runoff or subsurface storm flow (Freeze, (4)). It should be remarked that there are two views as for the variable source area concept; i.e. v.s.a.-overland-flow concept and v.s.a.-subsurface storm flow concept. According to the former view, a small part of the basin situated near stream head and along channel contributes to the surface runoff. While the latter concept asserts that the transfer of water from the hillslope to the stream is accomplished through subsurface routes by translatory flow. It should be remarked further that the v.s.a.-subsurface flow component of rainfall $x^{(2)}$, unlike the v.s.a.-overland flow, does not discharge immediately to the stream, but contribute to it according to the component unit-hydrograph of the interflow.

Since the inversely estimated inter-surface flow component of rainfall, $x^{(2)}$, is derived by considering that runoff occurs from the whole basin, the total amount of inter-surface flow rainfall is $Ax^{(2)}$. The actual process is illustrated schematically in Fig. 9. Therefore, the variable-source-area ratio (based on the v.s.a.-subsurface storm flow concept), $A_r = a/A$, is given by

$$Ar(t) = \frac{a}{A} = \frac{\hat{x}^{(2)}(t)}{X(t)-\hat{x}^{(1)}(t)} \qquad (12)$$

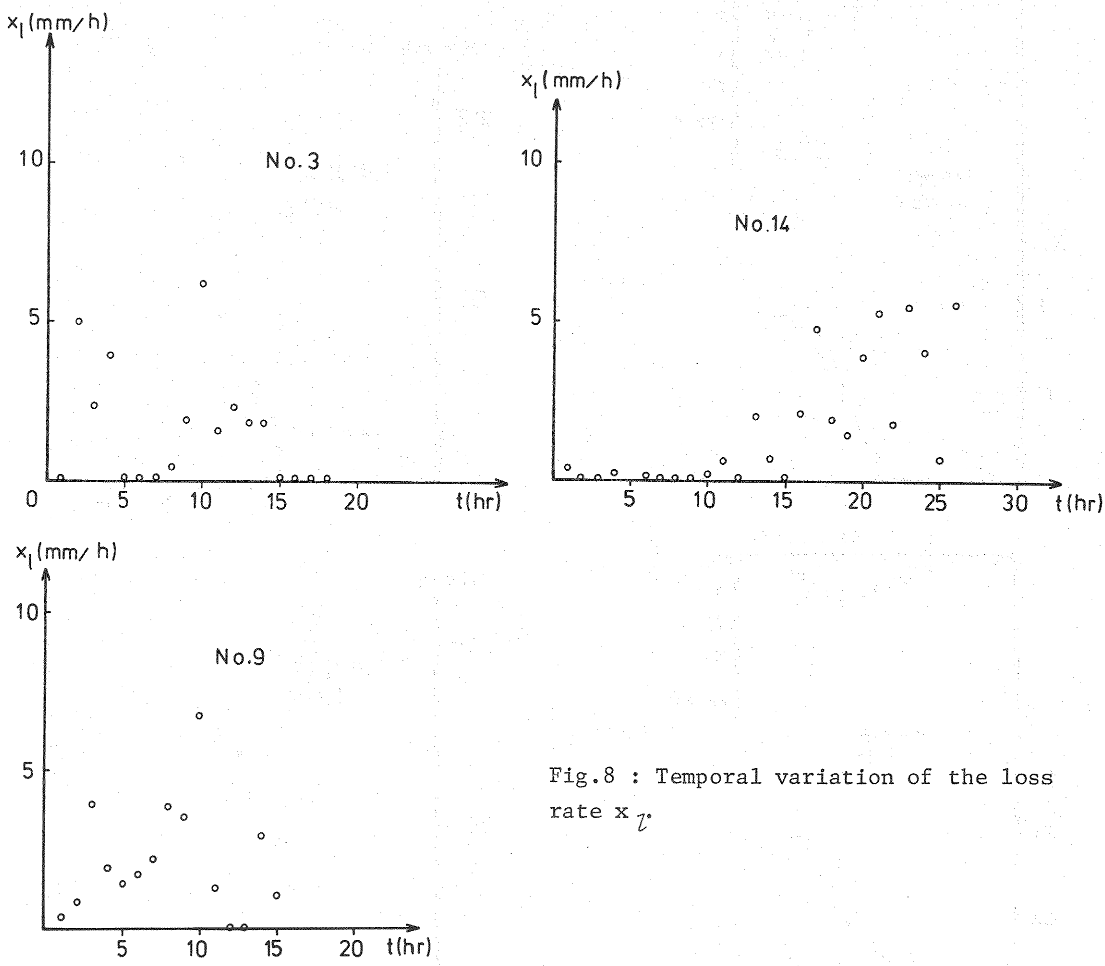

Fig.8 : Temporal variation of the loss rate x_l.

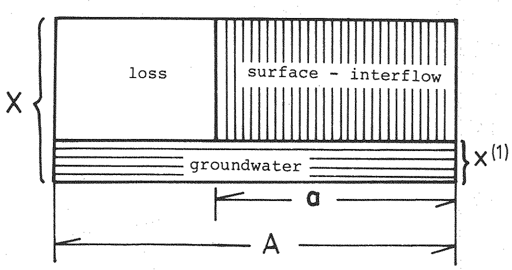

Fig.9 : Schematic representation of the "variable source area" concept.

The temporal changes of the variable-source-area ratio, Ar, are shown in Fig. 10, in which gradual and then rapid increase with time in Ar is given. A random variation of $x^{(2)}$ shown in Fig.6 is quite well explained by Fig.10. The ratio shown in the figure reaches a maximum value as high as Ar = 80%, a higher ratio compared with the generally supposed value for the v.s.a.-overland flow (for instance, compare Betson's (2) data). This will in turn prove the dominance of the variable source area-subsurface storm flow generation in this drainage basin.

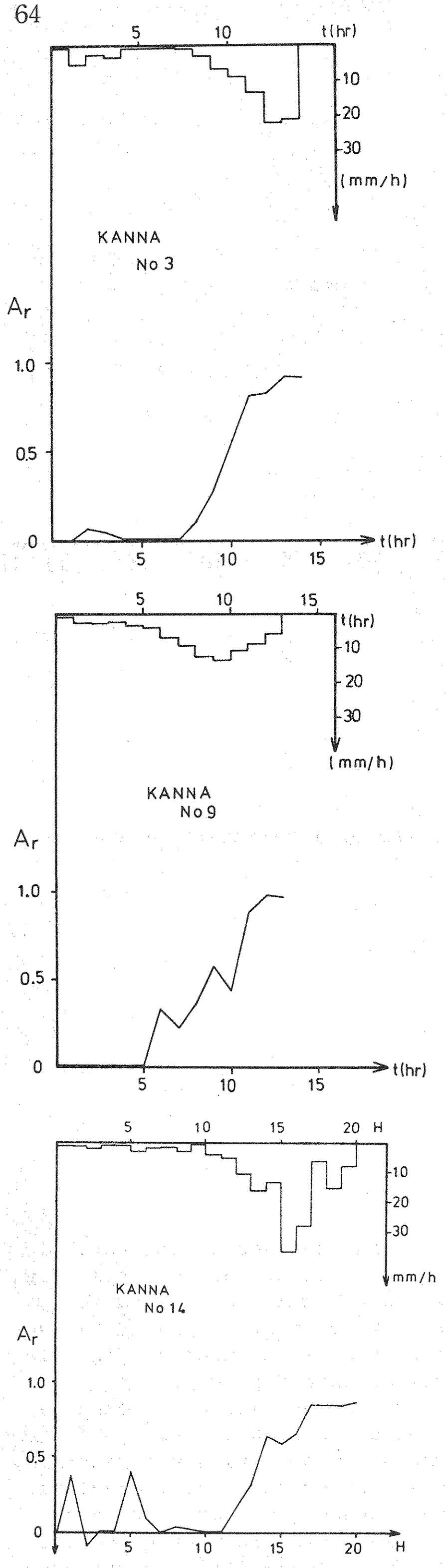

Fig.10 : Temporal change of the variable source area ratio, A_r, (of subsurface storm flow).

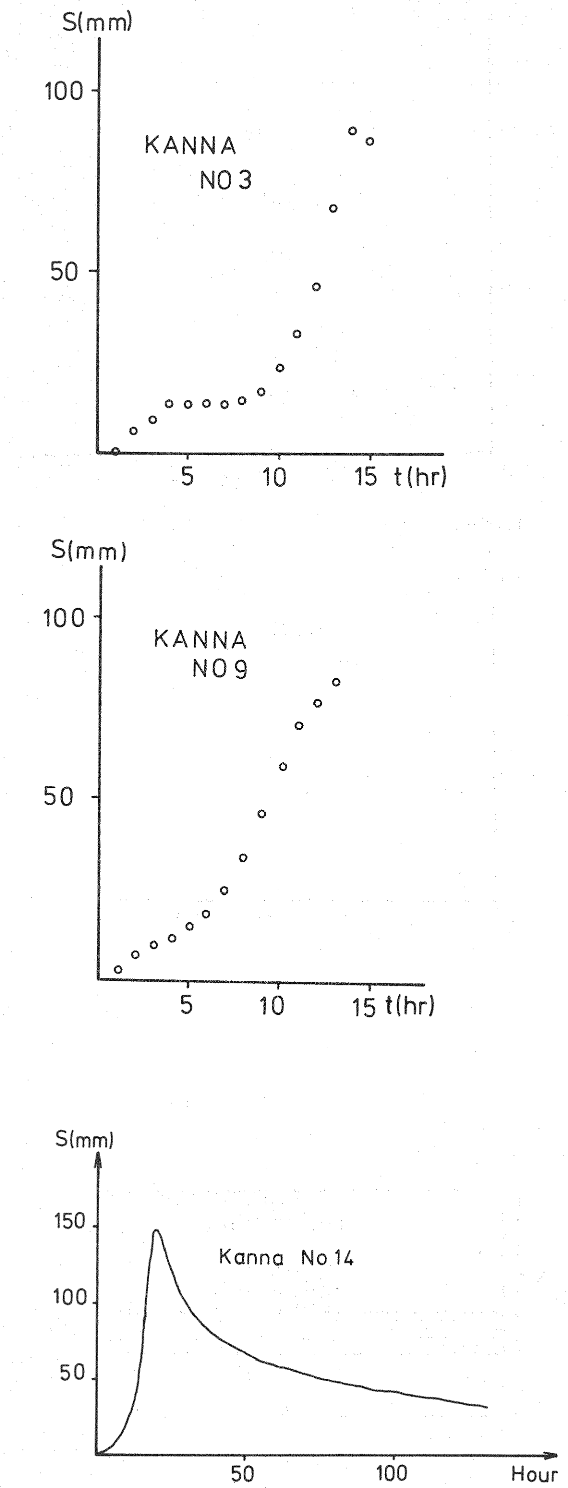

Fig.11 : Temporal change of the basin storage, S.

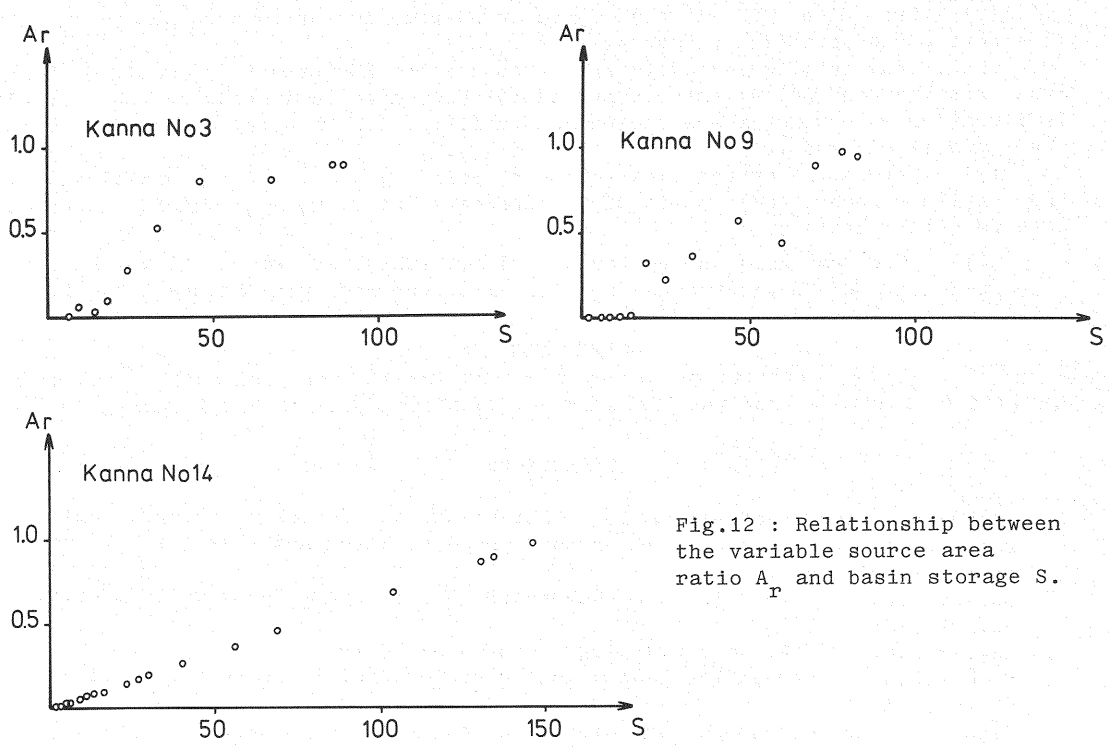

Fig.12 : Relationship between the variable source area ratio A_r and basin storage S.

Variable Source Area Ratio and Basin Storage

As might be soon imagined, the variable source area will increase depending on the basin storage S(t), which is estimated by

$$S(t) = \int_0^t (X(T)-Y(T))dt \fallingdotseq \sum (X_i - Y_i)\Delta t \tag{13}$$

where Y(t) and Y_i are the observed runoff.

The temporal change of S is given in Fig.11 whose behavior is quite similar with that of A_r shown in Fig.10. Consequently, the variable source area ratio A_r is plotted against storage S (Fig.12) , to show that A_r increases in proportion to S,

$$A_r = fn(S) \propto S \tag{14}$$

Rewritting Eq. (12), $x_s(=x^{(2)})$ is given by

$$x_s(t) = A_r(S)(X(t)-x_G(t)) \tag{15}$$

CONCLUSIONS

Analysing the component-rainfall time series which is inversely estimated from raw runoff time series by the filter-separation AR method, the nonlinear rainfall-separation law is derived.

(1) The groundwater component of rainfall, $x^{(1)}(=x_G)$, increases initially with the effective rainfall x until a certain limit $(x^{(1)})_f(=(x_G)_f)$ is reached.

(2) The final infiltration rate into groundwater subsystem $(x_G)_f$ is dependent on the preflood discharge rate q_A.

The final infiltration rate into groundwater subsystem $(x_G)_f$ defined here must not be confused with the conventional Hortonian definition of the final infiltration rate which means the maximum infiltration velocity of rainfall into the surface soil and is far greater than $(x_G)_f$.

(3) The inter-surface flow component rainfall $x^{(2)}(=x_s)$ is explained by the variable source area ratio of subsurface storm flow, A_r, which increases with rainfall duration.

(4) The variable source area ratio of subsurface storm flow, A_r, is proportional to the basin storage S which also increases with rainfall duration.

ACKNOWLEDGEMENT

This work has been supported by a Grant-in-Aid for Scientific Research (No.5846016, M.Hino) from the Ministry of Education, Science and Culture.

REFERENCES

1. Amorocho,J. and Brandstetter,A, : Determination of nonlinear functional response functions in rainfall-runoff process, Water Res. Res., vol.7, no.5, pp.1087-1101, 1971.
2. Betson,R.P., : 'What is watershed runoff?', J.Geophy. Res., vol.69, no.8, pp.1541-1552, 1964.
3. Eagleson,P.S. : Dynamic Hydrology, McGrow-Hill, 1970.
4. Freeze,R.A. : Streamflow generation, Rev. Geophys. Space Phys., vol.12, 627-647, 1974.
5. Hino,M. & Hasebe,M., : A hydrologic inverse problem: Analysis of rainfall-runoff characteristics and separation of runoff components from the discharge sequences, Proc.23rd Japanese Conference on Hydraulics, pp.193-198, JSCE (in Japanese), 1979.
6. Hino,M. & Hasebe,M., : Further test of applicability of the inverse detection method and extension to hourly hydrologic data, Proc. 3rd IAHR Symposium on Stochastic Hydraulics, Tokyo, pp.129-140, 1980.
7. Hino,M. & Hasebe,M., : Analysis of hydrologic characteristics from runoff data --- A hydrologic inverse problem, J. Hydrology, vol.49, pp.287-313, 1981.
8. Hino,M. & Hasebe,M. : Relation between runoff factor and antecedent discharge rate as an index of the humidity of a basin--Hourly data, Proc. Jpn. Soc. Civil Eng., No.328, pp.41-46 (English translation, Runoff ratio, rainfall intensity--Hourly data : J.Hydroscience and Hydraulic Eng., JSCE, vol.1, no.2, 1983), 1982.
9. Hino,M. & Hasebe,M. : Identification and prediction of nonlinear hydrologic systems by the filter-separation autoregressive (AR) method : Extension to hourly hydrologic data, J.Hydrology, vol.68, pp.181-210, 1984.
10. Hino,M. & Nadaoka,K., : Mathematical derivation of linear and nonlinear runoff kernels, Water Res. Res., vol.15, no.4, pp.918-928, 1979.
11. Hino,M., Sukigara,T. & Kikkawa H., : Nonlinear runoff kernels of hydrologic system, Proc. the 1st U.S.-Japan Seminar in Hydrology, pp.102-115. Water Resources Publication, Fort Collins, Colo, 1971.
12. Iwagaki,Y., : Fundamental studies on the runoff analysis by characteristics, Disaster Prevention Res. Inst., Bull.10, Kyoto Univ, 1955.
13. Iwai,S. & Ishiguro,M., : Applied Hydrologic Statistics, Morikita Pub. Co., Tokyo, p.342 (in Japanese), 1970.
14. Kikkawa, H., Sunada,K, & Nguyen,S.H., : Study on runoff model characteristics, Proc. Jpn. Soc. Civil Eng., no.283, pp.23-32, 1979.
15. Kimura,T., : Storage function method, Part III, Civil Eng. Journal, vol.4, no.4, pp.175-180, (in Japanese), 1962.
16. Kirkby,M.J.(Editor), : Hillslope Hydrology, John Wiley & Sons, 1978.
17. Linsley,Jr.R.K., Kohler,M.A. & Paulhus, J.L.H., : Applied Hydrology, McGraw-Hill, New York, N.Y, 1949.

18. Prasad,R., : A nonlinear hydrologic system response model, J.Hydraul. Div., Proc. Am. Soc. Civ. Eng., vol.93, no.HY4, pp.201-221, 1967.
19. Sugawara,M., : On the analysis of runoff structure about several Japanese rivers, Jpn. J of Geophysics, pp.1-76, 1961.
20. Sugawara,M., : Method of Runoff Analysis, Kyoritsu Pub. Co. (in Japanese), 1972.
21. Takenouchi,T., : Hydrologic Data Book of Kanna River, Inst. of Public Works and Construction, Ministry of Construction, 1962.
22. Yamada,T., Hino,M. and Fujita,K., : Mechanism of runoff in small test basins (plots), Proc. 26th Jpn. Conf. on Hydraulics, JSCE, pp.229-236 (in Japanese); English version, the role of infiltration in runoff, "Frontiers in Hydrology", 1982.

APPENDIX - NOTATION

The following symbols are used in this paper:

a	= variable source area;
A	= area of drainage basin;
$A_k^{(\ )}$	= AR coefficients for the -th component;
Ar	= variable source area ratio = a/A;
$b^{(l)}$	= AR coefficient for $x_i^{(l)}$ for the -th component; ($b = 1 - a_1 - a_2 - \cdots - a_p$);
c_1, c_2	= constants, Eq.(3);
$h_k^{(l)}$	= unit hydrograph for the l-th component;
l	= number of the rainfall-runoff subsystems; i.e. $l=1$ is the groundwater subsystem, $l=2$ is the inter-surface flow subsystem;
p	= order of the AR model;
q_A	= preflood discharge rate;
S	= basin storage;
t	= time;
T_c	= time constant of runoff component separation;
$w(\tau)$	= numerical separation filter;
x_i	= inversely estimated rainfall, Eq.(11);
$x_i^{(l)}$	= inversely estimated rainfall component of the l-th component; for time step i, Eqs.(9) and (10);
x_s	= rainfall component for the surface runoff ($=x^{(2)}$);
x_g	= rainfall component for the groundwater flow ($=x^{(1)}$);
x_l	= rainfall loss rate;
X_i	= observed total rainfall;
$y_i^{(l)}$	= runoff component of the l-th component; and
Y_i	= observed total runoff.